

## Metallization of the Resistivity Tensor in $\text{Bi}_2\text{Sr}_2\text{CaCu}_2\text{O}_x$ through Epitaxial Intercalation

X.-D. Xiang, W. A. Vareka, A. Zettl, J. L. Corkill, and Marvin L. Cohen

*Department of Physics, University of California at Berkeley,  
and Materials Sciences Division, Lawrence Berkeley Laboratory, Berkeley, California 94720*

N. Kijima and R. Gronsky

*Department of Materials Science and Mineral Engineering, University of California,  
and National Center for Electron Microscopy, Materials Sciences Division, Lawrence Berkeley Laboratory,  
Berkeley, California 94720*

(Received 13 August 1991)

We have used iodine intercalation to alter the interplane interaction and the anisotropic resistivity tensor of the oxide superconductor  $\text{Bi}_2\text{Sr}_2\text{CaCu}_2\text{O}_x$ . Real-space transmission electron microscopy images confirm that iodine is epitaxially intercalated between the Bi-O bilayers. In the normal state above  $T_c$ , the metallic  $\text{CuO}_2$  plane sheet resistance is unaffected by intercalation, while the out-of-plane conduction is dramatically changed from semiconductorlike to metalliclike. This result is inconsistent with some of the theoretical predictions based on holon-spinon scattering.

PACS numbers: 74.70.Jm, 74.70.Vy, 74.65.+n

The unusual normal-state properties of high- $T_c$  copper oxides have been the focus of many theoretical studies. It has been claimed [1] that clarifying the nature of the normal state could be the key to understanding the mechanism of high- $T_c$  superconductivity in these materials. Various theories [2] have been proposed which differ in their descriptions of the normal state, e.g., the conduction mechanisms between and within the  $\text{CuO}_2$  planes and their role in high- $T_c$  superconductivity.

A dramatic feature of copper oxide superconductors is their electrical transport anisotropy. The normal-state in-plane resistivity typically varies linearly with temperature, whereas the out-of-plane resistivity almost universally displays semiconductorlike behavior [3]. In addition, the ratio of the out-of-plane to in-plane resistivities can be as high as 10000. An important issue [4] is whether these anisotropies arise from the intrinsic nature of the  $\text{CuO}_2$  network and are intimately related to  $T_c$ , or if they are just a consequence of the intermediate layer structure between  $\text{CuO}_2$  planes with no direct relation to the superconductivity mechanism.

Recently it was demonstrated [5,6] that intercalation can induce well-defined structural changes in superconducting oxides. For example, in the stage-I iodine-intercalated  $\text{IBi}_2\text{Sr}_2\text{CaCu}_2\text{O}_x$  ( $\text{IBi-2:2:1:2}$ ) compound, the intercalated iodine atoms cause a 23% expansion of the crystal along the  $c$  axis and a suppression of the bulk superconducting transition temperature by  $\approx 10$  K. X-ray studies [5] suggest that the iodine intercalates between the Bi-O bilayers, thus affecting the interlayer coupling but leaving the intrinsic  $\text{CuO}_2$  plane structure of the  $\text{Bi}_2\text{Sr}_2\text{CaCu}_2\text{O}_x$  ( $\text{Bi-2:2:1:2}$ ) host intact. This implies that the intercell coupling contribution to  $T_c$  in  $\text{Bi-2:2:1:2}$  is about 10 K. Further evidence is provided by the observation [6] that there is only a 5-K reduction in  $T_c$  for stage-II iodine-intercalated  $\text{Bi-2:2:1:2}$ , in which iodine

atoms intercalate into every other Bi-O bilayer.

In this Letter, we confirm the structure and report the first anisotropic transport measurements for the stage-I iodine-intercalation compound  $\text{IBi-2:2:1:2}$ . In the normal state above  $T_c$ , intercalation is found to have no effect on the  $\text{CuO}_2$  plane sheet resistance of the host  $\text{Bi-2:2:1:2}$  material, but it results in a "metallization" of the out-of-plane electrical conduction. Our results are directly relevant to the above issues of interplanar coupling and the superconductivity mechanism.

Single crystals of pristine  $\text{Bi-2:2:1:2}$  were intercalated with iodine using a gas-diffusion method described earlier [5]. The typical sample dimensions were 1.5 mm  $\times$  1.0 mm  $\times$  0.02 mm. X-ray diffraction confirmed the stage-I structure, and magnetization measurements showed  $T_c$  to be 80 K, consistent with previous studies [5]. Careful checks were performed to verify that the  $\sim 10$  K depression in  $T_c$  (compared to pristine  $\text{Bi-2:2:1:2}$ ) was due strictly to iodine insertion (and not, say, the "anneal schedule" used during the gas-diffusion process). In addition, to verify that the crystals were uniformly intercalated, an intercalated sample was multiply cleaved and each section was examined by x-ray diffraction. The data for each section were consistent with stage-I  $\text{IBi-2:2:1:2}$  and showed no trace of the pristine phase.

To unambiguously determine the locations of the "guest" iodine species in the intercalated structure, crystals of pristine  $\text{Bi-2:2:1:2}$  and intercalated  $\text{IBi-2:2:1:2}$  were ion milled and examined in the JEOL JEM ARM-1000 atomic-resolution microscope using a through-focus series of phase-contrast images [7]. This transmission-electron-microscopy (TEM) method derives sufficient contrast to directly image the heavier cations, but not the lighter oxygen atoms. Figure 1(a) shows the atomic-resolution image of pristine  $\text{Bi-2:2:1:2}$ , viewed along the [110] direction; Fig. 1(b) shows a corresponding com-

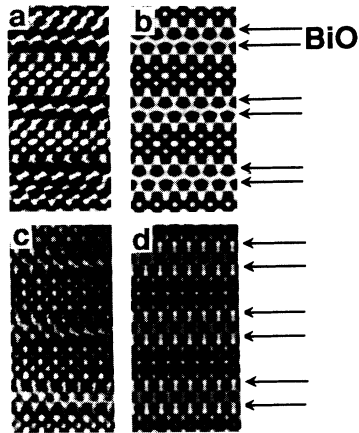


FIG. 1. Phase-contrast images of pristine and iodine-intercalated crystals. (a) Experimental micrograph of pristine Bi-2:2:1:2, (b) simulated micrograph of Bi-2:2:1:2, (c) experimental micrograph of intercalated IBi-2:2:1:2, and (d) simulated micrograph of intercalated IBi-2:2:1:2. The horizontal arrows identify Bi-O planes, between which iodine is located in the intercalated samples.

puter-generated image based on the well-known pristine Bi-2:2:1:2 structure. Note that from this viewing angle, the Bi atoms in adjacent Bi-O layers (identified by horizontal arrows) are staggered. Figure 1(c) is the atomic-resolution image of IBi-2:2:1:2, which clearly shows an expansion of the Bi-O bilayers and the positions of the iodine atoms intercalated between the Bi-O bilayers. In addition, intercalation shifts adjacent  $\text{CuO}_2$ -plane-containing blocks into common registry, thereby removing the staggered Bi sequence observed in pristine Bi-2:2:1:2. Comparison between images recorded under [010] and [100] directions demonstrates that the iodine is located between the oxygen atoms in the sandwiching layers; therefore, the iodine is epitaxially intercalated. Although only a few atomic layers are shown in Fig. 1(c), the actual micrographs cover much larger areas ( $> 1000 \text{ \AA}$ ), and confirm that long-range iodine order persists, consistent with x-ray studies. Figure 1(d) shows a computer-generated image [corresponding to Fig. 1(c)] assuming epitaxial iodine intercalation with a 23%  $c$ -axis expansion (3.6  $\text{\AA}$  per Bi-O bilayer), and a shift into common registry of adjacent  $\text{CuO}_2$ -containing blocks. Both x-ray and electron-microscopy results suggest that iodine intercalation has little effect on the internal structure of the pristine "blocks" that contain the  $\text{CuO}_2$  planes.

The anisotropic electrical resistivity  $\rho$  was measured using standard four-terminal methods [8] (employing silver or platinum paint contacts) and a contactless rf technique [9]. In the contactless rf technique, the sample was placed between two small coaxial coils, where one coil launched a 50-MHz signal and the other coil detected the signal transmitted through the sample. The transmission amplitude was then used to determine the

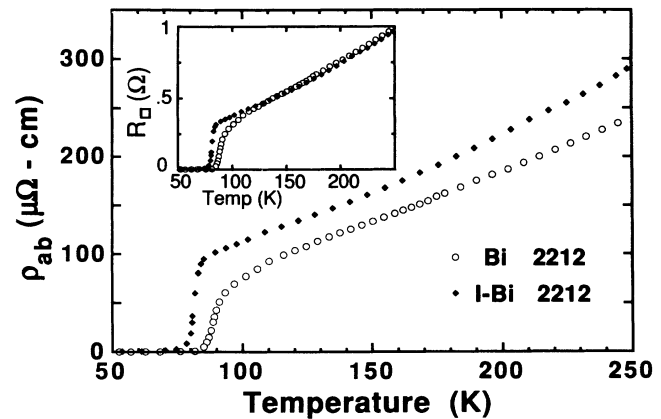


FIG. 2. In-plane resistivity for the same crystal before (Bi-2:2:1:2) and after (IBi-2:2:1:2) intercalation. Inset: The crystal sheet resistance  $R_{\square}$  before and after intercalation.

$ab$ -plane sheet resistance of the crystal. The contactless technique has the advantage that it measures true bulk sheet resistance without being sensitive to surface conditions or contact geometries; it is well suited to a precise measurement of the in-plane resistivity of the *same* crystal before and after intercalation.

Figure 2 shows the in-plane resistivity  $\rho_{ab}$  for a given crystal before (Bi-2:2:1:2) and after (IBi-2:2:1:2) iodine intercalation, obtained using the contactless rf technique. For Bi-2:2:1:2 (open circles),  $\rho_{ab}$  displays the roughly linear temperature dependence in the normal state above  $T_c$ , as observed in many previous studies. For the same sample after intercalation (solid diamonds),  $\rho_{ab}$  shows a qualitatively similar behavior, except that, compared to pristine Bi-2:2:1:2, the magnitude of  $\rho_{ab}$  is slightly larger and  $T_c$  is somewhat depressed (consistent with magnetization studies). There also appears to be a slight change in slope in  $\rho_{ab}$  for IBi-2:2:1:2 near  $T \sim 180 \text{ K}$ .

Since intercalation expands the  $c$  axis of Bi-2:2:1:2 by 23%, an increase in  $\rho_{ab}$  upon intercalation is expected even in the absence of any change in the conduction properties of the  $\text{CuO}_2$  planes (these planes are assumed to dominate the in-plane conduction). The inset to Fig. 2 shows for the same crystal the in-plane sample resistance (i.e., crystal sheet resistance,  $R_{\square}$ ) before and after intercalation. Over much of the normal-state temperature range,  $R_{\square}$  is nearly identical for Bi-2:2:1:2 and IBi-2:2:1:2. Careful checks indicate that the magnitudes of  $R_{\square}$  for Bi-2:2:1:2 and IBi-2:2:1:2 agree to within 1% at room temperature (we note that possible errors in measurement of the sample thickness do not affect this result, since this dimension does not enter the analysis for  $R_{\square}$  in the contactless resistance technique). We thus conclude that the difference in  $ab$ -plane resistivity between Bi-2:2:1:2 and IBi-2:2:1:2 is a consequence only of the crystal expansion; *conduction along the  $\text{CuO}_2$  planes is virtually unaffected by the intercalation.* On the other hand,

as we show below, intercalation dramatically changes the out-of-plane conduction.

Figure 3 shows the  $c$ -axis resistivity  $\rho_c$  as a function of temperature for a pristine Bi-2:2:1:2 crystal and an iodine intercalated IBi-2:2:1:2 crystal. Numerous pristine and intercalated specimens were measured using both the Montgomery contact geometry [8] and a large-area current and small-area voltage pad geometry with similar results. For pristine Bi-2:2:1:2 (open circles),  $\rho_c$  shows the "semiconductorlike" temperature dependence characteristic of out-of-plane transport for this and related materials. Although the increase in  $\rho_c$  with decreasing temperature has a complicated temperature dependence, it is often referred to as "1/ $T$ -like." The solid diamonds in Fig. 3 are for IBi-2:2:1:2. In sharp contrast to the semiconductorlike temperature dependence observed in the pristine material,  $\rho_c$  for the intercalated crystal shows an absolutely linear temperature dependence over the entire normal-state range. Given that  $\rho_{ab}$  is not changed by intercalation and that TEM, electron diffraction, and visual inspection do not show any intercalation-induced defects which could couple the  $ab$ -plane into the  $c$ -axis measurement, we conclude that this temperature dependence in  $\rho_c$  is intrinsic and not due to a "tortuous path" conduction as may occur in intercalated graphite [10]. Hence, intercalation changes the semiconductorlike or 1/ $T$ -like behavior for  $\rho_c$  into metalliclike.

Although the temperature dependence of the resistivity tensor in IBi-2:2:1:2 is metalliclike for both in-plane and out-of-plane transport, it is important to note that the in-plane to out-of-plane conduction anisotropy remains extreme. Indeed, as Fig. 3 demonstrates, the rough order of magnitude of  $\rho_c$  well above  $T_c$  is quite comparable for pristine and intercalated specimens.

There have been several predictions of the normal- and superconducting-state behavior of the layered oxides by Wheatley, Hsu, and Anderson (WHA) [11,12] and by Anderson and Zou (AZ) [13], all based on a model derived from the resonating-valence-bond theory. The ex-

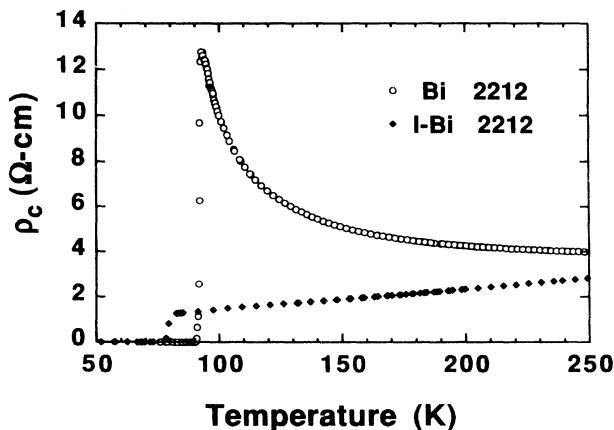


FIG. 3. Out-of-plane resistivity vs temperature for typical pristine (Bi-2:2:1:2) and intercalated (IBi-2:2:1:2) crystals.

perimental studies presented here can be used to examine these predictions and to provide information about microscopic interactions in these systems. Any viable model must account for both the small shift in  $T_c$  and the dramatic change in out-of-plane conduction induced by intercalation.

The observed change in  $T_c$  with intercalation is consistent with the WHA model of layered systems [11] if we assume that the next-nearest  $\text{CuO}_2$  plane coupling ( $\Lambda_o$ ) is essentially eliminated by iodine intercalation while the nearest-plane coupling ( $\Lambda_m$ ) in the intercalated material is the same as in the pristine material since these planes are within a single block. The couplings  $\Lambda$  have the form

$$\Lambda_{o,m} \sim |T_{\perp o,m}|^2/J, \quad (1)$$

where  $|T_{\perp}|$  is the interlayer hopping matrix element for nearest-neighbor  $\text{CuO}_2$  planes ( $m$ ) and next-nearest-neighbor planes ( $o$ ), and  $J$  is the spinon bandwidth. If  $\Lambda_o \rightarrow 0$ , then either  $T_{\perp o} \rightarrow 0$  or  $J \rightarrow \infty$ . The spinon bandwidth  $J$  depends only on the structure of the spinon energy spectrum which in turn is determined solely by the  $\text{CuO}_2$  planes. The condition  $J \rightarrow \infty$  is not physical nor is it reasonable, as will be shown in the discussion of  $\rho_{ab}$  below. Thus, we are left with the conclusion that  $T_{\perp o} \rightarrow 0$ , or is at least greatly reduced.

We now examine the anisotropic electrical resistivity. In the AZ calculation, the resistivity in the  $ab$  plane is caused by the scattering of holons by spinons. Thus,  $\rho_{ab}$  is a probe of the in-plane interaction and the densities of states of the spinons and holons. Specifically [13],

$$\rho_{ab} = (m_B/n e^2) (2\pi/\hbar) t^2 g_s g_b T, \quad (2)$$

where  $m_B$  is the effective mass of the holons,  $n$  is the holon density,  $t$  is the in-plane scattering matrix element between holons and spinons, and  $g_s$  ( $g_b$ ) is the spinon (holon) density of states. The value of  $\rho_{ab}$  for the intercalated samples demonstrates that the resistance of the  $\text{CuO}_2$  planes is unchanged by the intercalation. Furthermore, the values of  $t$ ,  $g_s$ ,  $g_b$ , and  $J$  depend only on the spinon-holon local environment in the  $\text{CuO}_2$  planes, and would remain constant unless the intercalation affected the structure of the material in those planes. The near-plane interlayer hopping matrix element ( $T_{\perp m}$ ) also only depends on the local environment of the closest spaced  $\text{CuO}_2$  planes. Thus, we can assume that  $t$ ,  $J$ ,  $g_s$ ,  $g_b$ , and  $T_{\perp m}$  are not affected by the intercalation. This supports the proposition that  $\Lambda_m$  is not altered by the intercalation, and that the observed depression in  $T_c$  is due to a reduction in  $\Lambda_o$  through a decrease in  $|T_{\perp o}|$ .

The out-of-plane resistivity  $\rho_c$ , however, poses a problem to an interpretation based on the AZ calculation. Intercalated samples display a metallic  $\rho_c$  down to  $T_c$ . The AZ calculation for  $\rho_c$  in a single-plane system, following a similar development as for  $\rho_{ab}$ , gives [13]

$$\rho_c = \left[ \frac{\hbar}{2\pi e^2} \right] \left[ \frac{ab}{c} \right] \left[ \frac{1}{|T_{\perp}|^2 g_s g_b^2 T} \right], \quad (3)$$

where  $T_{\perp}$  is the interlayer matrix element for the scattering of spinons and holons,  $ab$  is the area of the Cu-Cu square in the  $ab$  plane, and  $c$  is the interlayer distance. Since in this interpretation Bi-2:2:1:2 should have two types of  $c$ -direction tunneling—from nearest-neighbor planes and next-nearest-neighbor planes—Eq. (3) is logically extended to give

$$\rho_c \sim 1/\alpha\Lambda_o T + 1/\beta\Lambda_m T, \quad (4)$$

where  $\alpha$  and  $\beta$  include factors of the densities of states,  $J$ , and the different  $c$ -axis spacings for nearest-neighbor and next-nearest-neighbor  $\text{CuO}_2$  planes.

In view of the  $T_c$  and  $\rho_{ab}$  measurements, if  $\Lambda_o$  decreases we would expect  $\rho_c$  for intercalated Bi-2:2:1:2 to have a dramatically *increased*  $1/T$ -like behavior, whereas experiment shows no evidence for *any*  $1/T$ -like behavior (see Fig. 3). In addition, the  $T_c$  measurements indicate [5] that  $\Lambda_m \approx 9\Lambda_o$ . Assuming the  $\Lambda_o$  term has been replaced by some other mechanism, with the appropriate temperature dependence, one would *still* expect to see a small  $1/T$  contribution to the resistivity from the  $\Lambda_m$  term near  $T_c$ . However, this is not observed experimentally.

In light of this inconsistency, the previously proposed model does not adequately explain the resulting  $\rho_c$  of the iodine intercalated Bi-2:2:1:2 material. In this theory, the description of the  $c$ -axis conductivity mechanism and the pairing interaction for the superconducting state (i.e.,  $T_{\perp}$ ) are intimately related, and the small change in  $T_c$  and the large effect on  $\rho_c$  cannot be self-consistently accounted for.

This work was supported by the Director, Office of Energy Research, Office of Basic Energy Sciences, Materials Sciences Division of the U.S. Department of Energy under Contract No. DE-ACO3-76SF00098. J.L.C. and

M.L.C. were also supported by NSF Grant No. DMR88-18404. J.L.C. acknowledges support from an NSF Graduate Fellowship and M.L.C. acknowledges support from the J. S. Guggenheim Foundation.

- 
- [1] P. W. Anderson and R. Schrieffer, *Phys. Today* **44**, No. 6, 54 (1991).
  - [2] *High Temperature Superconductivity*, edited by K. Bedell, D. Coffey, D. E. Meltzer, D. Pines, and R. Schrieffer (Addison-Wesley, Redwood City, CA, 1990).
  - [3] T. Ito, H. Takagi, S. Ishibashi, T. Ido, and S. Uchida, *Nature (London)* **350**, 596 (1991).
  - [4] See, for example, D. H. Lowndes, D. P. Norton, and J. D. Budai, *Phys. Rev. Lett.* **65**, 1160 (1990).
  - [5] X.-D. Xiang, S. McKernan, W. A. Vareka, A. Zettl, J. L. Corkill, T. W. Barbee, III, and M. L. Cohen, *Nature (London)* **348**, 145 (1990); X.-D. Xiang, W. A. Vareka, A. Zettl, J. L. Corkill, and M. L. Cohen, *Phys. Rev. B* **43**, 11496 (1991).
  - [6] X.-D. Xiang, A. Zettl, W. A. Vareka, J. L. Corkill, T. W. Barbee, III, M. L. Cohen, N. Kijima, and R. Gronsky, (unpublished).
  - [7] N. Kijima, R. Gronsky, X.-D. Xiang, W. A. Vareka, A. Zettl, J. L. Corkill, and M. L. Cohen (unpublished).
  - [8] H. C. Montgomery, *J. Appl. Phys.* **42**, 2971 (1971).
  - [9] T. Sakakibara, T. Goto, and N. Miura, *Rev. Sci. Instrum.* **60**, 444 (1989).
  - [10] I. L. Spain, in *The Physics of Semimetals and Narrow-Gap Semiconductors*, edited by D. L. Carter and R. T. Bate (Pergamon, New York, 1971), p. 177.
  - [11] J. M. Wheatley, T. C. Hsu, and P. W. Anderson, *Nature (London)* **333**, 121 (1988).
  - [12] J. M. Wheatley, T. C. Hsu, and P. W. Anderson, *Phys. Rev. B* **37**, 5897 (1988).
  - [13] P. W. Anderson and Z. Zou, *Phys. Rev. Lett.* **60**, 132 (1988).

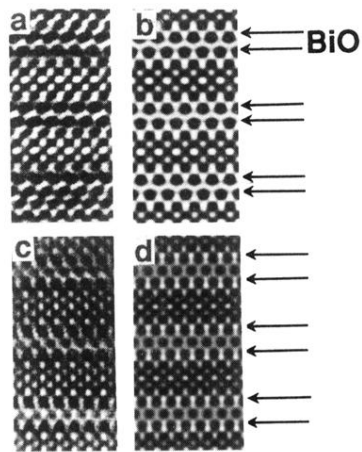


FIG. 1. Phase-contrast images of pristine and iodine-intercalated crystals. (a) Experimental micrograph of pristine  $\text{Bi-2:2:1:2}$ , (b) simulated micrograph of  $\text{Bi-2:2:1:2}$ , (c) experimental micrograph of intercalated  $\text{IBi-2:2:1:2}$ , and (d) simulated micrograph of intercalated  $\text{IBi-2:2:1:2}$ . The horizontal arrows identify Bi-O planes, between which iodine is located in the intercalated samples.